Interaction between tectonics and climate encoded in the planform geometry of stream networks on the eastern Tibetan Plateau

Minhui Li[1, 2], Hansjörg Seybold[2], Baosheng Wu[1], Yi Chen[1] and James W. Kirchner[2, 3, 4]

[1] State Key Laboratory of Hydroscience and Engineering, Tsinghua University, Beijing, China

[2] Department of Environmental Systems Science, ETH Zurich, Zurich, Switzerland

[3] Swiss Federal Research Institute WSL, Birmensdorf, Switzerland

[4] Department of Earth and Planetary Science, University of California, Berkeley, CA, USA

Corresponding author: Baosheng Wu (baosheng@tsinghua.edu.cn)

Key Points:

- Branching angles of major stream networks on the eastern Tibetan Plateau vary systematically with climatic aridity and channel slopes.
- Climatic controls dominate over tectonic drivers in shaping the branching angles in the flat interior of the eastern Tibetan Plateau.
- Tectonic controls dominate over climate in shaping the branching angles in the steep margin of the eastern Tibetan Plateau.

Abstract

Stream networks are highly abundant across Earth's surface, reflecting the tectonic and climatic history under which they have developed. Recent studies suggest that branching angles are strongly correlated with climatic aridity. However, the impact of tectonic forcing, especially in tectonically active regions, remains ambiguous. Here we analyze the branching angles of major stream networks on the eastern Tibetan Plateau, a region with complex tectonics, variable climate, and diverse landscapes. We find that spatial variations in tectonic uplift (as reflected in channel gradients) shape the branching geometry of stream networks on the steep eastern margin while in the flat interior of the eastern Tibetan Plateau, branching angles are mainly controlled by climatic aridity. This leads to the conclusion that, in the steep margin of the eastern Tibetan Plateau, climatic impacts on branching angles are overprinted by stronger tectonic controls.

Plain Language Summary

The geometry of stream networks reflects the tectonic and climatic evolution of a landscape. Prior studies show that stream branching angles tend to be wider in wetter climates. However, branching angles are also shaped by topography and thus by tectonic forcing, and the importance of climate relative to tectonics is not clear. Here we analyze branching angles of major stream networks on the eastern Tibetan Plateau, a tectonically active region where climatic aridity and channel slopes vary systematically from the relatively flat, dry interior to the steep, wet margin. The results show that stream network branching angles reflect the joint influence of tectonic forcing and climate. In the flat interior, branching angles are wider in wetter climates, consistent with previous studies in other regions. However, in the steep eastern margin, branching angles become narrower as climate becomes wetter and topographic gradients simultaneously become steeper. The shift in the relationship between angles and climatic aridity is observed in the transitional zone at intermediate topographic slopes. These results indicate that climatic controls on branching angles are gradually overwhelmed by tectonic controls as one goes from the relatively flat terrain of the interior to the steeper terrain of the tectonically active eastern margin.

1. Introduction

Numerous studies suggest that Earth's topography is shaped by the interplay between climate and tectonic forcing (Whittaker, 2012). River systems, for example, adjust their planform and profile geometry in response to erosion and uplift, and thus record information about a landscape's evolutionary past (Kwang et al., 2021; Perron et al., 2012; Seybold et al., 2021). Exploring the drivers that control the morphology of river systems can therefore provide insights into the processes that have shaped Earth's surface.

The branching angle formed by two incoming tributaries is a key morphological attribute that characterizes the planform geometry of stream networks. Thus, it may be diagnostic for the erosion processes at play and reveal how these processes vary across different tectonic and climatic zones. Recent studies have shown that mean branching angles are strongly related to climatic aridity not only across the United States (Getraer & Maloof, 2021; Seybold et al., 2017) but also globally (Seybold et al., 2018). Branching angles are typically narrower in arid regions than in humid climates, potentially indicating differences in the dominant erosion mechanisms across different climates (Seybold et al., 2017). Two distinct channel-forming processes that contribute to the headward growth of stream networks have been suggested: channel incision by surface runoff (Horton, 1945) and diffusive processes such as groundwater seepage (Dunne, 1990). Overland flow occurs when rainfall exceeds soil infiltration capacity and thus the water is routed downhill along the line of steepest descent. This phenomenon was first described by Horton (1945). Horton also observed that streams with a greater difference in slopes are more likely to branch at wider angles, consistent with steepest-descent routing of each tributary (Getraer & Maloof, 2021; Horton, 1945). Headward erosion by groundwater seepage was extensively studied by Dunne in the early 90s (Dunne, 1990). Recent theoretical studies have suggested that valley heads formed by re-emerging groundwater flow should tend to bifurcate at a characteristic angle of $\alpha = 2\pi/5 = 72°$. This theoretical prediction is consistent with field measurements in a valley network on the Florida panhandle that is known to be formed by groundwater seepage (Devauchelle et al., 2012; Petroff et al., 2013).

Erosion is shaped by both climatic and tectonic forcing (Hurst et al., 2019; Whittaker, 2012), and it has been widely recognized that gradients in precipitation control spatial variations in erosion rates in regions with relatively uniform tectonically-driven rock uplift rates (Ferrier et al., 2013; Henck et al., 2011; Reiners et al., 2003). In contrast, uplift and hillslope processes become major drivers of erosion rates in tectonically active margins (Harkins et al., 2007; Vance et al., 2003), potentially shaping networks' drainage patterns. Surface slope for example plays an important role in determining drainage patterns (Howard, 1967; Zernitz, 1932). Drainage patterns that occur without pronounced structural or topographic controls tend to be dendritic, with tributaries joining at wide angles (Howard, 1967). In more narrowly spaced basins, parallel drainage patterns with narrower branching angles are more common, implying that

regional topographic gradients influence the network's geometry (Howard, 1967; Zernitz, 1932). Jung et al. (2011) observed a transition between dendritic and parallel patterns in both natural and simulated channel networks with regional surface slopes exceeding ~3%. In arid and semi-arid regions, however, preexisting slopes seem to have no significant influence on the development of parallel or pinnate networks (Jung & Ouarda, 2017). Across the United States, Seybold et al. (2017) observed that branching angles are systematically narrower in steeper terrain, although the correlation between branching angles and channel slopes is weaker than that with aridity. However, relationships between climatic aridity, channel slopes and branching angles in tectonically active areas are less clear.

In order to better understand the interplay between tectonic forcing and climate in shaping a stream network's geometry, we analyze the morphology of the river systems of the eastern Tibetan Plateau. The Tibetan Plateau is a particularly interesting study area due to its strong gradients in climate and surface uplift (Clark et al., 2004). The Tibetan Plateau is located in the southwestern part of China and is often referred to as the Third Pole (Qiu, 2008). It has formed primarily due to the collision and continued convergence between the Indian and Eurasian plates (Wu, Zuza, et al., 2019) and the eastward growth of the Tibetan Plateau is thought to be driven by crustal shortening or viscous lower crustal flow (Royden et al., 2008; Tapponnier et al., 2001). The growth of the Himalayas and the Tibetan Plateau accounts for the large-scale drainage patterns of most Asian river systems (Chen et al., 2021; Clark et al., 2004; Li et al., 2022; Yang et al., 2015) which cover a wide range of different landscapes in different climatic and tectonic zones. With an average elevation of more than 4000 m above sea level, the Tibetan Plateau acts as a barrier for westerlies and monsoon circulation (Zhao et al., 2022). These topographic conditions create large climatic gradients between the plateau's arid interior and its monsoon-influenced southeast margin (Hudson & Quade, 2013). The increased precipitation, from the flat interior to the highly dissected eastern margin, is generally accompanied by steeper terrain.

While the large climatic and tectonic gradients make the Tibetan Plateau a particularly interesting place for studying the influence of different controls on stream network formation, the strong coupling and feedbacks between climate and uplifted topography make it challenging to disentangle the different driving mechanisms. While our study focuses on the formation of stream network branching angles under the joint influence of climate and tectonic forcing on the eastern Tibetan Plateau, our results may also provide general clues for the development of stream networks in tectonically active regions.

2. Data and Methods

2.1. Stream Networks and Branching Angles

The Tibetan Plateau, known as the water tower of Asia, is the source of most of Asia's largest rivers (Immerzeel et al., 2010). Our study focuses on the river systems of the

eastern Tibetan Plateau, including the Yellow, Yangtze, Mekong and Salween Rivers, as well as the Yarlung (Tsangpo) River (Figure 1).

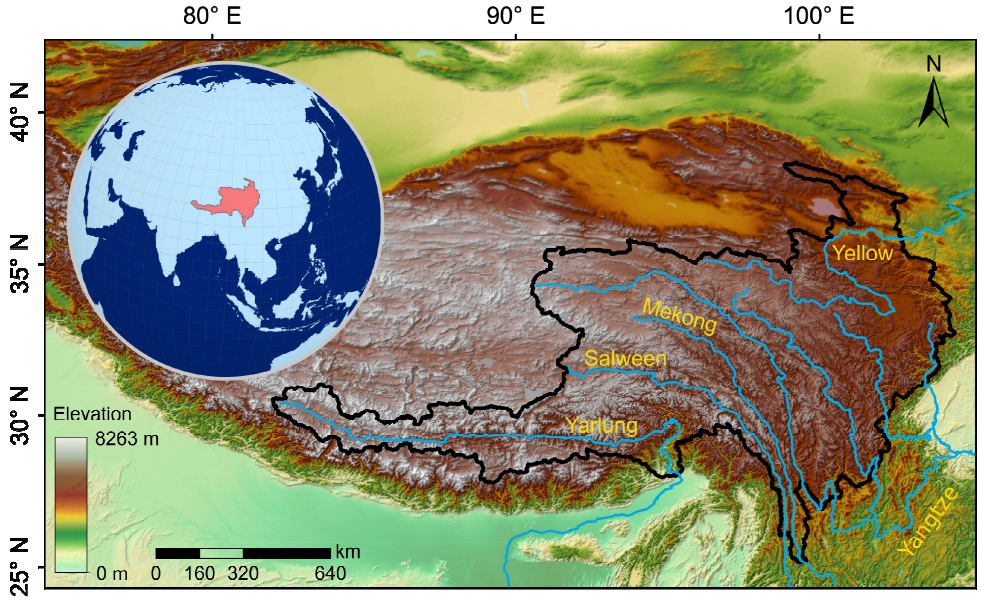

Figure 1. Context map of the Tibetan Plateau showing topography and major rivers (blue lines) in our study area, the boundary of which is denoted by a solid black line. The inset shows the location of the study area on the globe.

The stream networks analyzed in this study have been extracted from the 90-m-resolution Shuttle Radar Topography Mission Digital Elevation Model (SRTM-DEM) (https://search.earthdata.nasa.gov/search) using the code DEMRiver (Bai et al., 2015a; Wu, Li, et al., 2019). For the network extraction, we have set the critical source area (CSA) threshold to 40 pixels, corresponding to a drainage area of roughly 0.324 km^2. Several geometric properties of stream networks such as channel slopes and Horton-Strahler (H-S) order are included in the feature calculation. In addition to the stream network, DEMRiver also provides basins and sub-basins for the different river reaches using the hierarchical pyramid method of Bai et al. (2015b) (Figure S1 in Supporting Information S1).

The branching angle (α) between two upstream tributaries has been calculated following the approach described by Seybold et al. (2017), which includes the following four steps. (1) We re-project the drainage networks using a conformal (angle preserving) projection. Here we use a Lambert conformal cone. (2) The projected vector segments are then converted into a series of points ordered from upstream to downstream. (3) In the next step, we fit straight lines to the two upstream tributaries using orthogonal least squares. (4) Finally, we calculate the angle between the orientation of the two regression lines.

In our analysis, we excluded branching angles formed by channels with negative slopes, which account for roughly 9% of the dataset and are the result of the least-cost

routing scheme implemented in the DEMRiver program, which allows overcoming local depressions without elevation modification. We then averaged all the branching angles within level-5 basins. Among all level-5 basins, 215 basins containing less than 10 branching angles were removed from our statistics. These basins had average areas of 8 km^2 and mostly contained only two or three river segments. Finally, we end up with 3571 sub-basins containing a total of 789,175 branching angles. These basins have an average size of roughly ~300 km^2 and typically contain ~200 junctions.

2.2. Climatic and Tectonic Metrics

The Aridity Index (AI = *P*/PET) is often used to describe climatic conditions because it represents the balance between precipitation (*P*) and the evaporative demand of the atmosphere, as quantified by potential evaporation (PET). For our analysis of the eastern Tibetan Plateau, we calculated the mean AI value in each basin using the aridity data from the Global Aridity and PET Database (Trabucco & Zomer, 2018), which contains 30-year normals for the period 1970 to 2000 at a spatial resolution of 30 arc-seconds. Note, because AI is defined as the ratio of precipitation to potential evapotranspiration, higher values of AI mean more humid conditions.

Tectonic forcing can create topography and maintain relief through surface uplift. Widely used topographic metrics to characterize tectonic activity are mean hillslope gradients, local relief, and in fluvial landscapes, channel steepness (Whipple, 2004). Topographic slopes have been widely used as proxies of erosional response to spatial variations in tectonic uplift rates (Kirby & Whipple, 2012; Seybold et al., 2021; Whipple, 2004). Hillslope gradients are often used to characterize surface roughness but cease to provide a proxy for erosion at high rates (>~0.2 mm/a) because they reach the threshold of hillslope stability (Ouimet et al., 2009). By contrast, channel slopes can be more reliable erosion proxies in rapidly eroding landscapes, because they continue to steepen with increasing erosion rates. Therefore our analysis uses mean topographic slope (S_t) to quantify the roughness of topography and classify the eastern Tibetan Plateau into different zones, and uses channel slope (S_c) to quantify the impact of tectonic activity on stream networks' mean branching angles.

3. Results and Discussion

3.1. Spatial Patterns in Branching Angles, Climate and Tectonics on the Tibetan Plateau

The spatial distributions of basin-wide averaged aridity index (AI), topographic slope (S_t), and branching angles (α) are shown in Figure 2 (left column) together with their kernel density distributions (Figure 2, right column). Regional patterns are clearly visible, with AI values varying between 0.15 in the dry northwestern part of the eastern Tibetan Plateau and 2.96 at the most humid southeastern plateau margin (Figure 2a). Here, the deep valleys cut by the Yarlung and Salween Rivers serve as moisture paths for the South Asian Monsoon (Chen et al., 2021).

The deep gorges and steep rivers in the southern and eastern parts of the Tibetan Plateau reflect large gradients in exhumation rates (Wang et al., 2015; Yang et al., 2015). In the whole study area, topographic slopes and channel slopes vary widely and are highly correlated with each other (Spearman ρ = 0.983, $p < 0.01$). Topographic slopes average 16° and can reach up to 37° while channel slopes vary up to 23°. Except for the poorly drained low-relief areas of the Ruoergai Basin near the first bend of the Yellow River, topographic slopes tend to increase from the northwest to the southeast (Figure 2b). In the relatively low-relief interior of the Tibetan Plateau, comprising mainly the headwater areas of the Yellow, Yangtze, Mekong, and Salween Rivers, and in the Ruoergai Basin, topographic slopes are usually smaller than 7°. Conversely, topographic slopes increase to over 20° near the eastern plateau margin (Figure 2b). This high spatial variability in topographic and channel slopes also reveals the tectonic diversity of the region. On the southeastern margin of the Tibetan Plateau, Asia's big rivers have carved deep valleys into the uplifting bedrock. Deeply incised gorges and very steep rivers often coexist, which is related to zones of rapid rock uplift and incision (Hodges et al., 2001; Wang et al., 2015). In the Tsangpo Gorge, for example, the channel drops by almost ~2 km in a stretch of less than ~50 km (Wang et al., 2015).

Basin-averaged branching angles in the flat and dry interior, and in the headwaters of the Yarlung River, tend to be systematically narrower than in other regions of the study area. Additionally, the widest branching angles tend to occur in the transitional zone between the interior and the margin of the eastern Tibetan Plateau (Figure 2c). From the transitional zone towards the southeastern margin of the Tibetan Plateau, branching angles become narrower although climatic aridity AI increases. This suggests that branching angles on the eastern Tibetan Plateau may be the result of climatic signals superimposed on tectonic drivers.

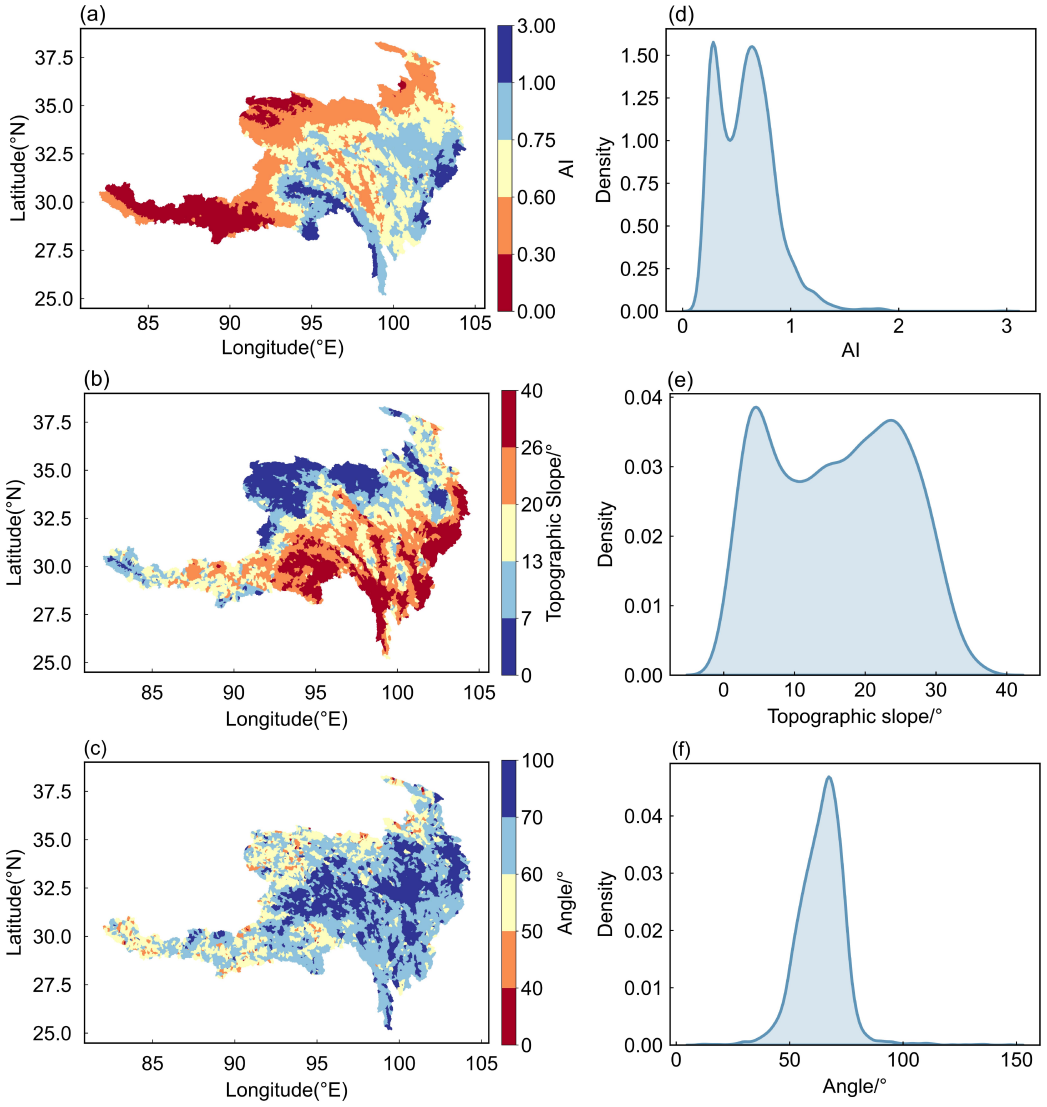

Figure 2. Spatial distributions of (a) basin-averaged aridity index (AI), (b) topographic slopes (S_t) and (c) basin-averaged branching angles (α) across our study area. AI and S_t generally increase from northwest to southeast, reflecting more humid climates and steeper landscapes in the southeast. Branching angles in the headwater reaches of the major rivers are usually narrower than in the other parts. Panels (d-f) show the corresponding kernel density distributions for AI, S_t, and α.

To explore the interdependence of branching angles, climatic aridity (here quantified by the aridity index AI), and tectonic forcing (here proxied by channel slope S_c), we first analyzed how branching angles vary with AI alone (Figure 3a). Here we averaged the basin values into bins that each contain ~2% of the data, and colored each point to reflect the average channel slope in each bin. Average branching angles increase systematically with increasing humidity (AI values of up to ≈ 0.75), and then start to decrease as AI increases further. From Figure 3a we see that these humid (high-AI)

basins also tend to have steep channel slopes, reflecting their proximity to the steep southeast margin of the Tibetan Plateau. A similar pattern is seen in the relationship between branching angles and channel slopes (Figure 3b), where again each point represents the binned mean of 2% of the data, and is colored to reflect the average AI in each bin. In Figure 3b, mean branching angles first increase with increasing channel slopes (as AI increases, reflecting increasing humidity), then decrease with increasing channel slopes (as AI remains high near the southeast margin of the Plateau). These general relations also persist after removing side-branches (Text S1 and Figure S2 in Supporting Information S1). These observations lead to the hypothesis that strong differences in topographic uplift caused by the collision of the Indian and Eurasian plates become a significant driver of the planform geometry of stream networks in the wet and steep part of the eastern Tibetan Plateau.

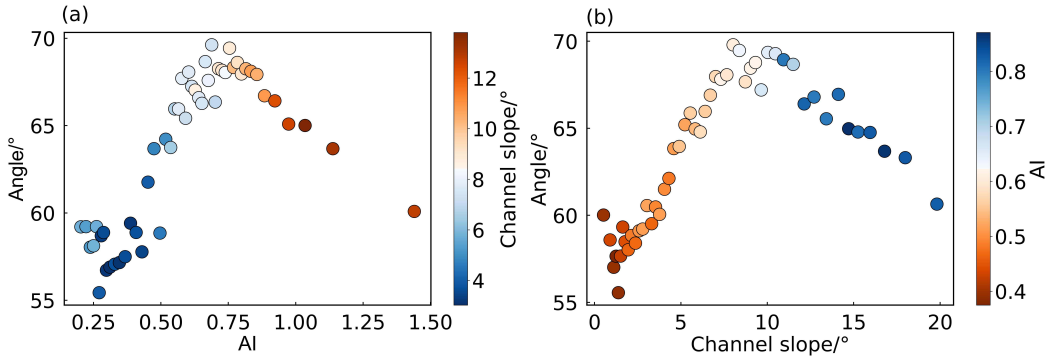

Figure 3. Relationships between mean branching angle and (a) aridity index AI or (b) channel slope (S_c). Each point contains ~2% of the whole data. The color gradient in (a) shows the variation of the average slope S_c, and in (b) it shows the variation in AI from dry (red colors) to humid (blue colors). Branching angles increase with increasing AI up to AI ≈ 0.75 and decrease as AI increases further, but points with high AI also have high S_c. A similar pattern is found in the relationship between branching angle and channel slopes: branching angles first increase with increasing S_c (as AI increases), and then decrease with increasing S_c (while AI remains high).

3.2. Climatic and Tectonic Controls on Branching Angles in Different Slope Classes

To disentangle the joint influence of climate and tectonic forcing, we divide our dataset into three zones based on topographic slope S_t. Each zone has been selected to contain roughly the same number of basins, namely 1165 basins for $S_t \leq 11°$, 1406 basins for $11° < S_t \leq 23°$ and 1000 basins with $S_t > 23°$. The flat catchments are generally located in the arid (mean AI = 0.44) interior of the eastern Tibetan Plateau, while the steep catchments are found along the humid (mean AI = 0.79) plateau margins, and the transitional catchments have intermediate climate (mean AI = 0.58) and are typically found between the flat and steep zones (Figure 4a). The kernel density distributions of AI and branching angles in the three different zones are shown

in Figures 4b and 4c respectively. Branching angles systematically increase with AI (Spearman ρ = 0.31 and 0.48 respectively, p < 0.001, Figure 4d) in the flat and transitional catchments. By contrast, the steep catchments exhibit a systematic decrease of α with AI (Spearman ρ = -0.24, p < 0.001) and a strong negative correlation between α and channel gradient (Spearman ρ = -0.48, p < 0.001, Table S1 in Supporting Information S1). These results suggest that the channel slope effect on branching angles overprints climatic controls in the steep and tectonically active terrain of the eastern Tibetan Plateau.

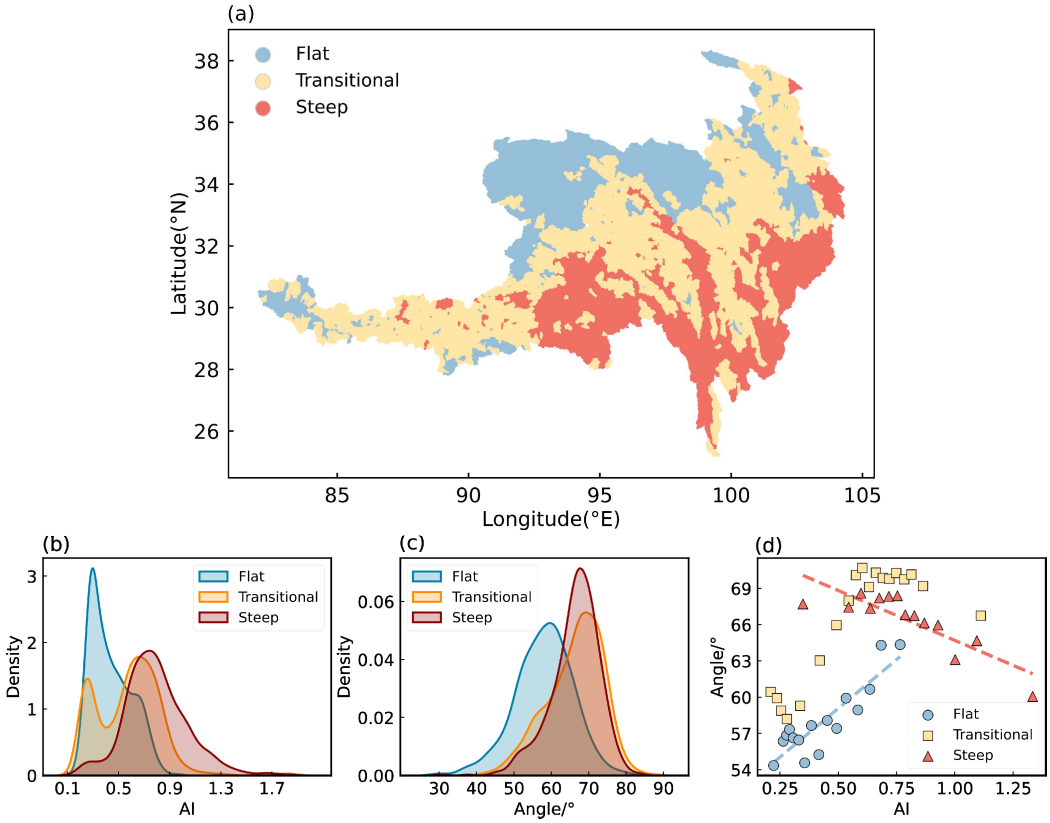

Figure 4. (a) Spatial distributions of three topographic slope classes: flat (blue), transitional (yellow) and steep (red). The classification roughly follows a trend from northwest to southeast. (b and c) Kernel density estimate plots of aridity index AI and branching angle α. (d) Relationships between the basin-averaged α and AI in the three different topographic slope classes. In the flat catchments, found primarily in the interior of the Tibetan Plateau, α systematically increases with AI, while the steep catchments, found primarily along the southeast margin of the Plateau, show a systematic decrease of α with AI.

The relationship between AI, channel slopes (S_c) and branching angles (α) can also be quantified by a multiple regression model,

$$\alpha = \beta_0 + \beta_1 \mathrm{AI} + \beta_2 S_c + \beta_3 (\mathrm{AI} \cdot S_c) \quad (1)$$

where the branching angle α is approximated as a linear function of AI, S_c, and their interaction (denoted by AI · S_c), with β_i indicating the regression coefficients. We used z-scores of each variable in Equation (1) and applied this model to the whole study area, and also separately to the flat, transitional, and steep catchments.

Across the dataset as a whole, we find that AI and channel slopes are strongly interdependent (Spearman ρ= 0.527, $p < 0.001$), and thus their interaction term has a strong effect on the overall relationship between branching angles and climatic (AI) and tectonic (S_c) influences. Across our whole study area, AI and channel slope account for roughly 30% of the observed variance in basin-averaged branching angles (Table 1). While AI and channel slopes are positively correlated with branching angles, the regression coefficient of their interaction term is strongly negative, and this negative effect may reverse the apparent correlation that one sees when branching angles are plotted as functions of AI or channel slope alone. AI has the strongest control on basin-averaged branching angles (β = 0.79, $p < 0.001$) in the flat catchments but does not significantly influence branching angles in the steep catchments (β = -0.07, $p > 0.1$). Conversely, in the steep catchments, channel slope is the dominant factor (β = -0.43, $p < 0.001$) in controlling the networks' branching angles and thus overprints the positive relationship between branching angles and AI. The interaction term between AI and channel slopes is insignificant in both the flat and steep topography classes (Table 1), with $p > 0.1$. These results indicate that the interaction effect of AI and channel slopes is weaker (and thus the effects of AI and channel slopes are more clearly expressed) when flat and steep catchments are considered separately.

Table 1. Multiple regression parameters for the whole Eastern Tibetan Plateau dataset (ETP) and different topographic slope classes. Regression parameters with $p < 0.001$ are shown in italics.

	ETP	Flat	Transitional	Steep
AI	*0.37*	*0.79*	*0.42*	-0.07
S_c	*0.24*	-0.19	*0.25*	*-0.43*
AI · S_c	*-0.46*	0.27	*-0.51*	-0.10
R-squared	0.304	0.117	0.256	0.253

4. Conclusions

In this study, we evaluated the relative dominance of climatic aridity and channel slope in shaping the branching angles of stream networks on the eastern Tibetan Plateau. Our analysis shows that spatial patterns in average branching angles reflect spatial gradients in climatic aridity and channel slope. On the eastern Tibetan Plateau,

the correlation between branching angles and climatic aridity reverses between the relatively flat interior and the steep eastern margin. In the flat interior, branching angles primarily reflect variations in climatic aridity, consistent with prior studies. Going from the flat interior to the steep margin, tectonic forcing becomes increasingly important as a control on branching angle variability, leading to an inverse correlation between branching angles and climatic aridity. These findings demonstrate the joint influence of tectonic forcing and climate in shaping river network morphology.

Acknowledgments

This study was partly supported by the National Natural Science Foundation of China (No. 51639005). Minhui Li acknowledges support from the Chinese Scholarship Council.

Data Availability Statement

The dataset used to produce our results is accessible in Data at https://figshare.com/articles/dataset/Branching_angles_on_ETP_csv/21728126.

References

Bai, R., Li, T. J., Huang, Y. F., Li, J. Y., & Wang, G. Q. (2015a). An efficient and comprehensive method for drainage network extraction from DEM with billions of pixels using a size-balanced binary search tree, *Geomorphology*, *238*, 56-67.

Bai, R., Li, T. J., Huang, Y. F., Li, J. Y., Wang, G. Q., & Yin, D. Q. (2015b). A hierarchical pyramid method for managing large-scale high-resolution drainage networks extracted from DEM, *Computers & Geosciences*, *85*, 234-247.

Chen, Y., Wu, B., Xiong, Z., Zan, J., Zhang, B., Zhang, R., et al. (2021). Evolution of eastern Tibetan river systems is driven by the indentation of India, *Communications Earth & Environment*, *2*(1), 1-7.

Clark, M. K., Schoenbohm, L. M., Royden, L. H., Whipple, K. X., Burchfiel, B. C., Zhang, X., et al. (2004). Surface uplift, tectonics, and erosion of eastern Tibet from large-scale drainage patterns, *Tectonics*, *23*(1).

Devauchelle, O., Petroff, A. P., Seybold, H. F., & Rothman, D. H. (2012). Ramification of stream networks, *Proceedings of the National Academy of Sciences of the United States of America*, *109*(51), 20832-20836.

Dunne, T. (1990). Hydrology, mechanics, and geomorphic implications of erosion by subsurface flow, *Groundwater geomorphology: The role of subsurface water in earth-surface processes and landforms*, *252*, 1-28.

Ferrier, K. L., Huppert, K. L., & Perron, J. T. (2013). Climatic control of bedrock river incision, *Nature*, *496*(7444), 206-+.

Getraer, A., & Maloof, A. C. (2021). Climate-Driven Variability in Runoff Erosion Encoded in Stream Network Geometry, *Geophysical Research Letters*, *48*(3).

Harkins, N., Kirby, E., Heimsath, A., Robinson, R., & Reiser, U. (2007). Transient fluvial incision in the headwaters of the Yellow River, northeastern Tibet, China, *Journal of Geophysical Research-Earth Surface*, *112*(F3).

Henck, A. C., Huntington, K. W., Stone, J. O., Montgomery, D. R., & Hallet, B. (2011). Spatial controls on erosion in the Three Rivers Region, southeastern Tibet and southwestern China, *Earth and Planetary Science Letters*, *303*(1-2), 71-83.

Hodges, K. V., Hurtado, J. M., & Whipple, K. X. (2001). Southward extrusion of Tibetan crust and its effect on Himalayan tectonics, *Tectonics*, *20*(6), 799-809.

Horton, R. E. (1945). Erosional Development of Streams and Their Drainage Basins - Hydrophysical Approach to Quantitative Morphology, *Geological Society of America Bulletin*, *56*(3), 275-370.

Howard, A. D. (1967). Drainage analysis in geologic interpretation: a summation, *Aapg Bulletin*, *51*(11), 2246-2259.

Hudson, A. M., & Quade, J. (2013). Long-term east-west asymmetry in monsoon rainfall on the Tibetan Plateau, *Geology*, *41*(3), 351-354.

Hurst, M. D., Grieve, S. W. D., Clubb, F. J., & Mudd, S. M. (2019). Detection of channel-hillslope coupling along a tectonic gradient, *Earth and Planetary Science Letters*, *522*, 30-39.

Immerzeel, W. W., van Beek, L. P. H., & Bierkens, M. F. P. (2010). Climate Change Will Affect the Asian Water Towers, *Science*, *328*(5984), 1382-1385. doi: 10.1126/science.1183188.

Jung, K., & Ouarda, T. B. M. J. (2017). Classification of drainage network types in the arid and semi-arid regions of Arizona and California, *Journal of Arid Environments*, *144*, 60-73.

Jung, K. C., Niemann, J. D., & Huang, X. J. (2011). Under what conditions do parallel river networks occur? *Geomorphology*, *132*(3-4), 260-271.

Kirby, E., & Whipple, K. X. (2012). Expression of active tectonics in erosional landscapes, Journal of Structural Geology, 44, 54-75. doi: 10.1016/j.jsg.2012.07.009.

Kwang, J. S., Langston, A. L., & Parker, G. (2021). The role of lateral erosion in the evolution of nondendritic drainage networks to dendricity and the persistence of dynamic networks, *Proceedings of the National Academy of Sciences of the United States of America*, *118*(16).

Li, M. H., Wu, B. S., Chen, Y., & Li, D. (2022). Quantification of river network types based on hierarchical structures, *Catena*, *211*.

Ouimet, W. B., Whipple, K. X., & Granger, D. E. (2009). Beyond threshold hillslopes: Channel adjustment to base-level fall in tectonically active mountain ranges, *Geology*, *37*(7), 579-582. doi: 10.1130/g30013a.1.

Perron, J. T., Richardson, P. W., Ferrier, K. L., & Lapotre, M. (2012). The root of branching river networks, *Nature*, *492*(7427), 100-+.

Petroff, A. P., Devauchelle, O., Seybold, H., & Rothman, D. H. (2013). Bifurcation dynamics of natural drainage networks, *Philosophical Transactions of the Royal Society a-Mathematical Physical and Engineering Sciences*, *371*(2004).

Qiu, J. (2008). China: The third pole, *Nature*, *454*(7203), 393-396. doi: 10.1038/454393a.

Reiners, P. W., Ehlers, T. A., Mitchell, S. G., & Montgomery, D. R. (2003). Coupled spatial variations in precipitation and long-term erosion rates across the Washington Cascades, *Nature*, *426*(6967), 645-647.

Royden, L. H., Burchfiel, B. C., & van der Hilst, R. D. (2008). The geological evolution of the Tibetan plateau, Science, 321(5892), 1054-1058. doi: 10.1126/science.1155371.

Seybold, H., Rothman, D. H., & Kirchner, J. W. (2017). Climate's watermark in the geometry of stream networks, *Geophysical Research Letters*, *44*(5), 2272-2280.

Seybold, H., Berghuijs, W. R., Prancevic, J. P., & Kirchner, J. W. (2021). Global dominance of tectonics over climate in shaping river longitudinal profiles, *Nature Geoscience*, *14*(7), 503-+.

Seybold, H. J., Kite, E., & Kirchner, J. W. (2018). Branching geometry of valley networks on Mars and Earth and its implications for early Martian climate, *Science Advances*, *4*(6).

Tapponnier, P., Xu, Z. Q., Roger, F., Meyer, B., Arnaud, N., Wittlinger, G., & Yang, J. S. (2001). Geology - Oblique stepwise rise and growth of the Tibet plateau, *Science*, *294*(5547), 1671-1677.

Trabucco, A., & Zomer, R. J. (2018). Global aridity index and potential evapotranspiration (ET0) climate database v2, *CGIAR Consort Spat Inf*, *10*, m9.

Vance, D., Bickle, M., Ivy-Ochs, S., & Kubik, P. W. (2003). Erosion and exhumation in the Himalaya from cosmogenic isotope inventories of river sediments, *Earth and Planetary Science Letters*, *206*(3-4), 273-288.

Wang, P., Scherler, D., Liu-Zeng J., Mey, J., Avouac, J. P., Zhang, Y. D., & Shi, D. G. (2014). Tectonic control of Yarlung Tsangpo Gorge revealed by a buried canyon in Southern Tibet, *Science*, *346*(6212), 978-981.

Whipple, K. X. (2004). Bedrock rivers and the geomorphology of active orogens, *Annual Review of Earth and Planetary Sciences*, 32, 151-185. doi: 10.1146/annurev.earth.32.101802.120356.

Whittaker, A. C. (2012). How do landscapes record tectonics and climate? *Lithosphere*, *4*(2), 160-164.

Wu, C., Zuza, A. V., Zhou, Z. G., Yin, A., McRivette, M. W., Chen, X. H., et al. (2019). Mesozoic-Cenozoic evolution of the Eastern Kunlun Range, central Tibet, and implications for basin evolution during the Indo-Asian collision, *Lithosphere*, *11*(4), 524-550.

Wu, T., Li, J. Y., Li, T. J., Sivakumar, B., Zhang, G., & Wang, G. Q. (2019). High-efficient extraction of drainage networks from digital elevation models constrained by enhanced flow enforcement from known river maps, *Geomorphology*, *340*, 184-201.

Yang, R., Willett, S. D., & Goren, L. (2015). In situ low-relief landscape formation as a result of river network disruption, *Nature*, *520*(7548), 526-+.

Zernitz, E. R. (1932). Drainage patterns and their significance, *Journal of Geology*, *40*(6), 498-521.

Zhao, R., Fu, P., Zhou, Y., Xiao, X. M., Grebby, S., Zhang, G. Q., et al. (2022). Annual 30-m big Lake Maps of the Tibetan Plateau in 1991-2018, *Scientific Data*, *9*(1).